Probabilistic analysis of energy exchange processes for automotive hybrid powertrain

Miloš Milačić *, Chris Gearhart

Fuel Cell Center, Research & Advanced Engineering, Ford Motor Company, 1201 Village Rd, Dearborn, MI 48121, USA

ABSTRACT

In this paper a statistical method for establishing the minimum energy reservoir needed for a hybrid-electric vehicle (HEV) is proposed. This method is based on real world data and investigates the statistical properties of the charge and discharge events for a variety of driving profiles. The distribution of the magnitude of discharge and charge events was found to be exponentially distributed. Using an exponential distribution assumption, the probability distribution for the energy stored in the battery was calculated. This distribution is a function of only two parameters, the average discharge energy (μ_d), and the ratio of the average discharge energy to the average charge energy (ζ). These parameters are functions of the drive profiles of interest and the power-level of the HEV power supply. Based on this, a strategy HEV battery capacity and the power-level of the primary power supply was proposed. This strategy is of particular importance for fuel cell based HEVs because the cost of the fuel cell stack directly scales with the power level.

© 2011 Elsevier B.V. All rights reserved.

1. Introduction

The traditional engineering design approach is to design a system that meets requirements derived from a set of worst case scenarios. In design of hybrid vehicles there is an additional complexity added by determination of the degree of hybridization required (power ratio between primary source and energy reservoir) [1,2]. Such designs most often follow a "90-10 rule"—90% of the requirements can be met by a design that requires 10% of the resources, satisfying the last 10% of the requirements then uses the remaining 90% of the resources. Building in these performance reserves, while necessary in most cases, adds cost into the systems. Therefore, in setting system requirements it warrants asking *"How likely is this limiting requirement occurs? How much can we save if we accept a small probability of violating this requirement?"* This is an approach commonly used in robust design.

In this paper we present a robust design methodology that encompasses statistical aspects of the system requirements for battery sizing in automotive hybrid powertrains. Although not all automotive requirements can be compromised, some performance attributes do offer a potential of large savings with minor compromises in performance. The method described here relates to sizing of an energy reservoir which is depleted through a random process

and cannot be filled above a certain level. It will be demonstrated through an example of sizing hybrid powertrains (ICE[1] or fuel cell [3–8]) for automotive applications.

2. Problem statement, definitions and assumptions

For this analysis a simplified hybrid powertrain is assumed [7,9,10], shown in Fig. 1, that consists of a primary power source (internal combustion engine shown in Fig. 1(a)[10] or fuel cell shown in Fig. 1(b)[8]), an energy storage device (most likely a hybrid battery [11]) and a drivetrain (such as described in Ref. [12]). The power needed by the drivetrain to propel the vehicle is either generated by the primary source, or comes from the energy storage device, or some combination of those two. Several studies explored this energy flow as optimization process with goal of improved efficiency and fuel economy [13–15], while others focused on improvements in efficiency and fuel economy of the primary power source operation [16,17]. Unlike the optimization presented in [18] no battery chemistry nor demographic driver data were considered here. The question that we wish to answer is: *Given a distribution of driving scenarios, as the power required as a function of time, what must be the capacity of the battery to meet a specified fraction of the demand?* Furthermore, we can ask *how the capacity must change with the changes in the power rating of the primary power source?*

---

* Corresponding author. Tel.: +1 313 390 5474.
E-mail addresses: mmilacic@ford.com (M. Milačić), cgearha1@ford.com (C. Gearhart).

[1] ICE: Internal Combustion Engine.

(a) ICE Hybrid [10]

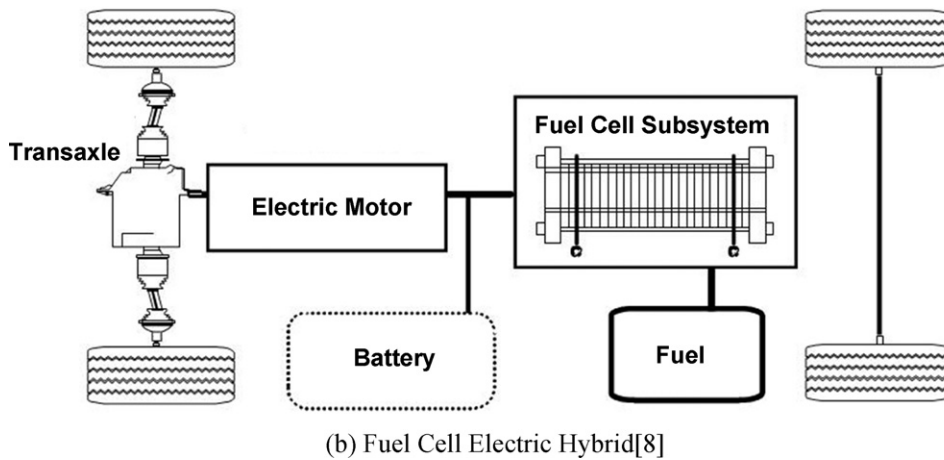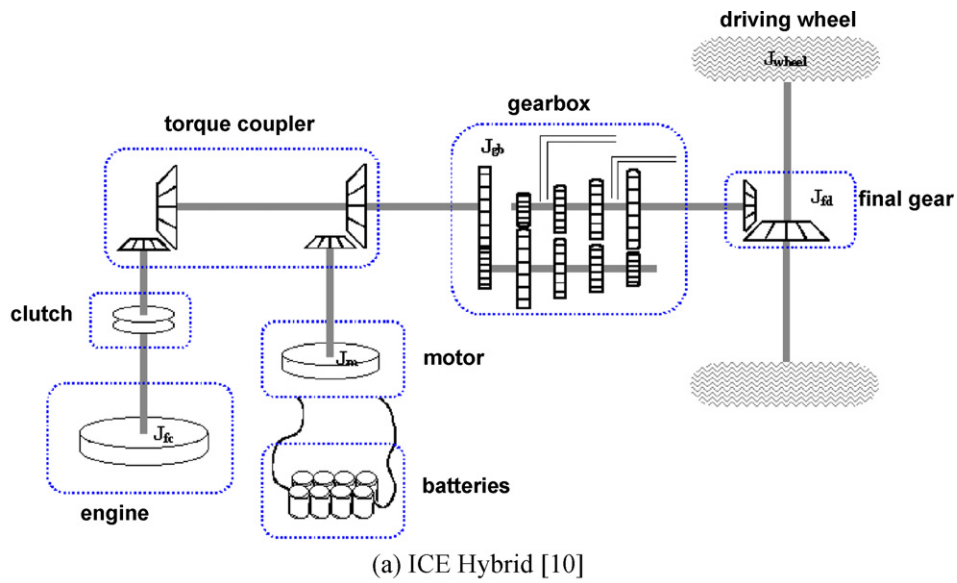

(b) Fuel Cell Electric Hybrid[8]

Fig. 1. Simplified hybrid powertrain architecture.

In order to answer these questions, several statistical variables were introduced (graphically explained in Fig. 3):

T_{above} — time above the threshold, $P(t) > P_H$

T_{below} — time below the threshold, $P(t) < P_H$

$$E_{above} = \int_{T_{above}} [P(t) - P_H] \, dt - \text{energy above } P_H$$

$$E_{below} = \int_{T_{below}} P(t) dt - \text{energy below } P_H$$

$$E_{fill} = \int_{T_{below}} [P_H - P(t)] \, dt - \text{energy available to charge}$$

where $P(t)$ is power required at time t, and P_H is the maximum power of the primary power source.

Conventional wisdom dictates that the power rating of the primary source has to be greater than the maximum power required by the vehicle. Questioning this approach the following sizing strategy questions were posed: *How small can the primary power source be made without changing the energy storage capacity required? If the primary source maximum power is P_H, how much energy would the energy storage device need to provide and for how long? Can*
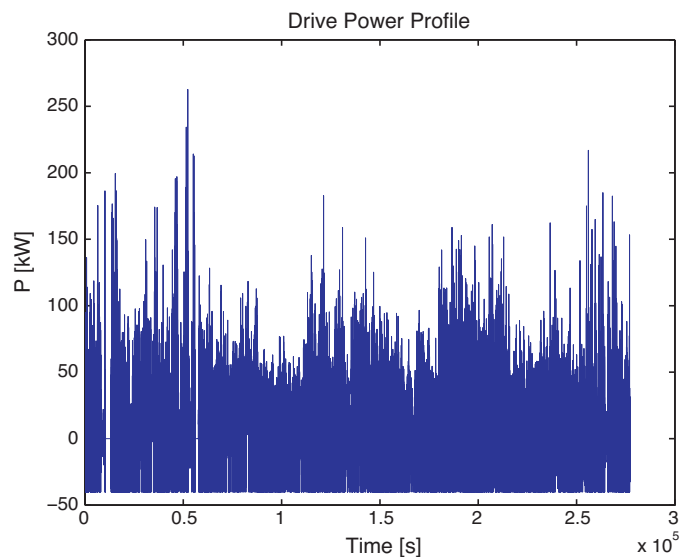

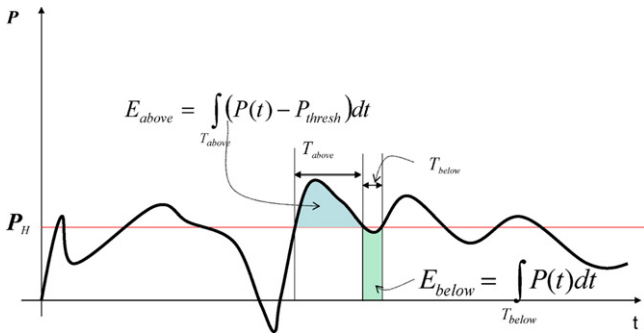**Fig. 2.** Overall drive power profile.

Fig. 3. Graphical representation of a drive trace with statistical variables shown.

the depleted energy from the energy storage device (eventually) be replenished?

3. Analysis

Using data from the drive trace shown in Fig. 2, for every value of P_H, distributions for T_{above}, E_{above}, T_{below}, and E_{fill} as function of P_H were generated. These are shown in Figs. 4 and 5, and are used

(a) Duration of P> P_H
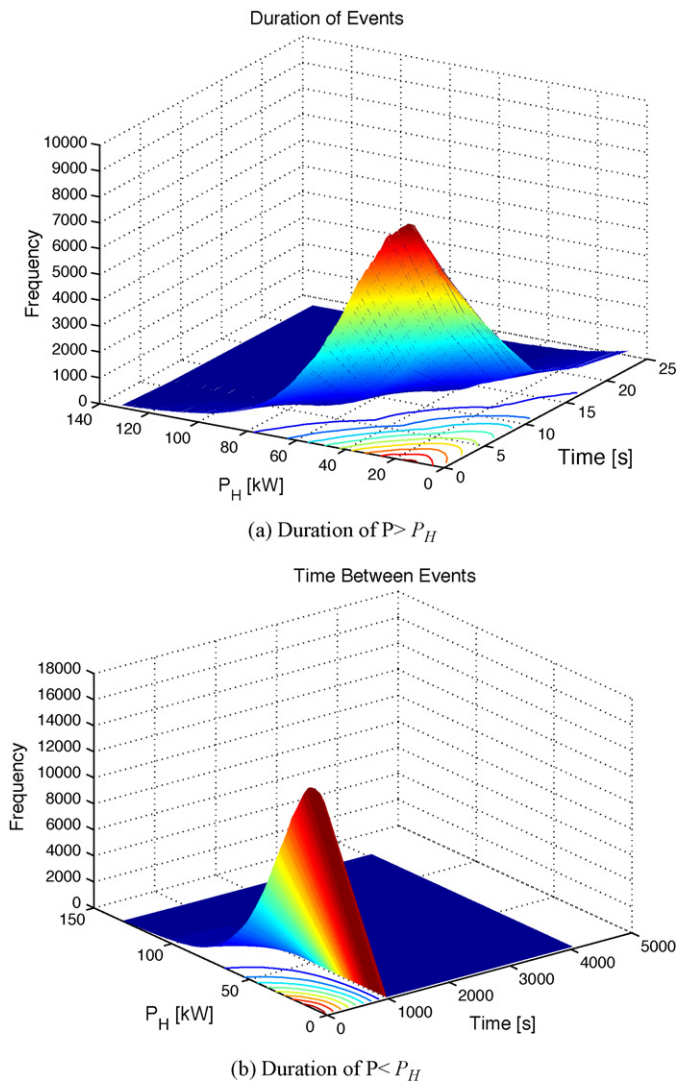
(b) Duration of P< P_H

Fig. 4. Temporal distributions for the driving profile. (a) Duration of $P > P_H$ and (b) duration of $P < P_H$.

(a) Energy content while P> P_H

(b) Excess Energy available while P< P_H
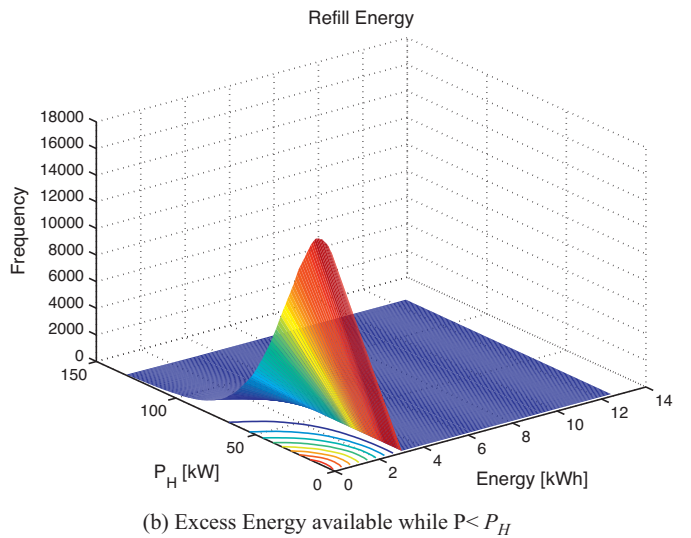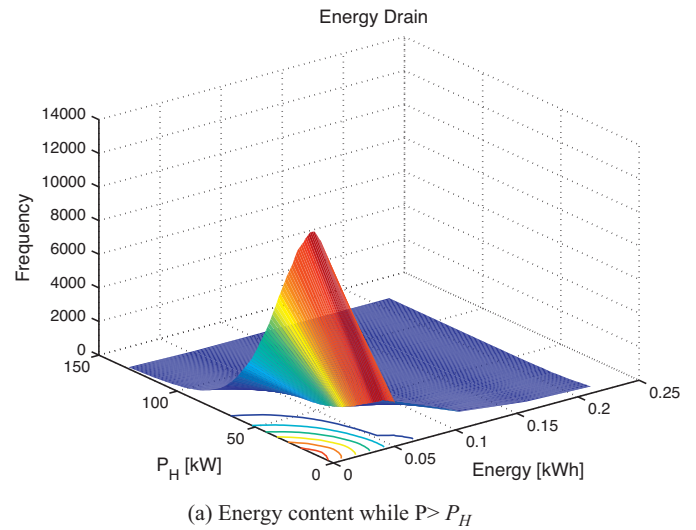
Fig. 5. Energy distributions for the driving profile. (a) Energy content while $P > P_H$ and (b) excess energy available while $P < P_H$.

to calculate the distribution of energy associated with charging and discharging events. These distributions are well approximated by exponential distributions with scale parameters μ_c, for charging events, and μ_d for discharging events. For the drive traces used in this paper, values of μ_c and μ_d, with their 95% confidence intervals, as function of P_H are shown in Fig. 6

3.1. Energy transfers

It can be assumed that the energy storage device (battery) is at initial state $E_0 = 0$. At any given time, the energy storage device is either discharging ($P > P_H$) or charging ($P < P_H$), assuming that threshold level P_H is the maximum power that primary source can supply. Although it is possible to have times during which the energy does not change, these "zero energy" transitions can be treated either as part of the previous or part of the following transition. Therefore, every charge event is followed and preceded by a discharge event, so we can graphically represent the energy history as shown in Fig. 7. This sequence of energy level transitions can be written as:

$$E_{k+1} = E_k + \Delta E_k. \tag{1}$$

(a) $\mu_c(P_H)$

(b) $\mu_d(P_H)$

Fig. 6. μ_c and μ_d (with 95% confidence intervals) for various P_H.

where:

$$\Delta E_k = \begin{cases} \Delta E_k > 0 \text{(charge)} & k = 2n \\ \Delta E_k < 0 \text{(discharge)} & k = 2n+1 \end{cases} \tag{2}$$

Fig. 7. Energy history with labeled transition orders.

The odd numbered energy levels in this sequence represent the energy depletion of the battery after each discharge event. The distribution of these energy levels tell us how frequently the ba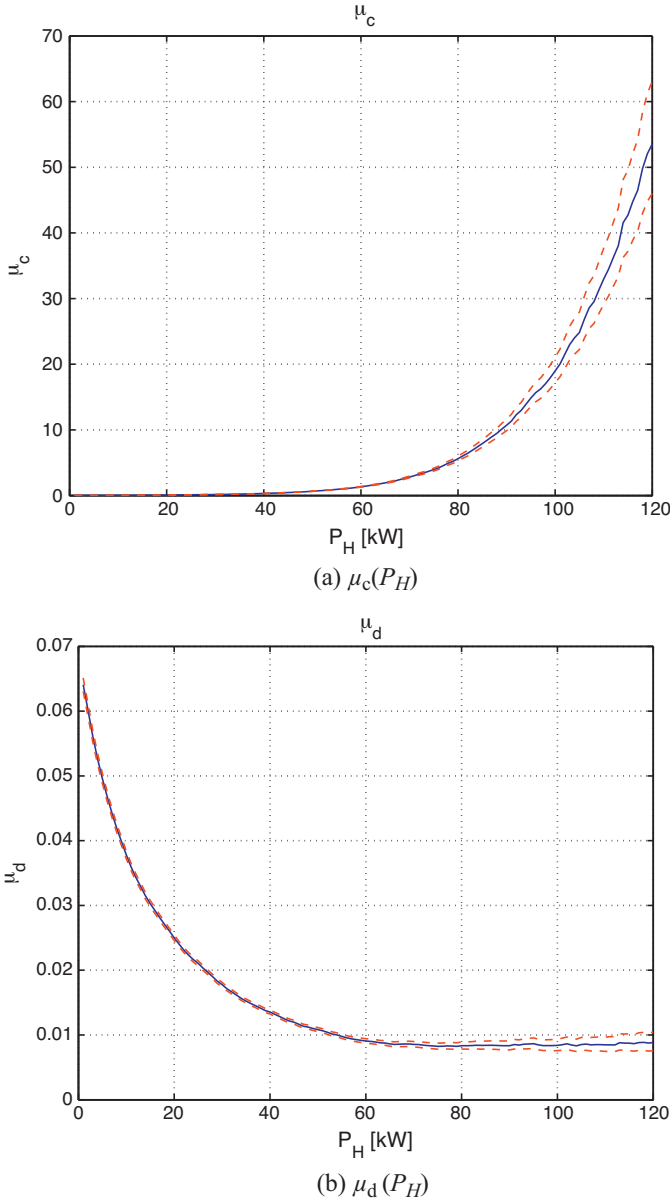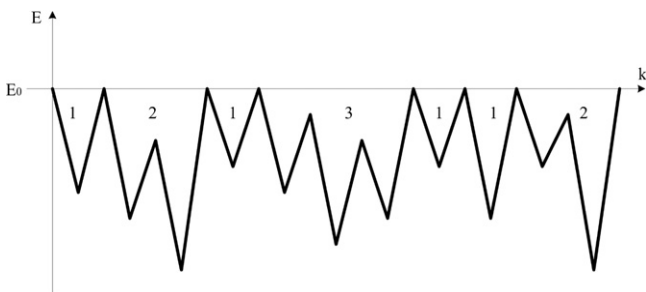ttery is discharged to a specific level. To calculate this distribution ($\hat{D}$) we calculate the distribution of energy levels associated with a single discharge event (D_1). To this we add the distribution of energy levels after three transitions (D_3) multiplied by the probability that the second transition did not replenish the battery (P_2) added by the distribution of energy levels after five transitions (D_5) multiplied by the probability that neither the second (P_2) nor the fourth transitions (P_4) replenished the battery, and so on. In expanded form:

$$\hat{D}(E) = D_1(E) + P_2(D_3(E) + P_4(D_5(E)\cdots)) = \sum_{i=0}^{\infty}\left(D_{2i+1}(E)\prod_{j=0}^{i}P_{2j}\right). \tag{3}$$

Now, the energy level distributions and energy transition probabilities are examined in more details. Keeping in mind that for a discharge event $\Delta E < 0$, the energy transition probability is given as:

$$P(\Delta E) = \frac{1}{\mu_d}e^{\Delta E/\mu_d}. \tag{4}$$

Similarly, the transition probability for a charge event ($\Delta E > 0$) is:

$$P(\Delta E) = \frac{1}{\mu_c}e^{-\Delta E/\mu_c}. \tag{5}$$

Before the discharge event $k = 2n$, it is assumed that the battery is at some energy level $\hat{E}$, that has the probability distribution $D_{2n}(E)$. After the discharge event, keeping in mind that $E < 0$, the energy distribution becomes:

$$\hat{D}_{2n+1}(E) = \int_{E}^{0} D_{2n}(\hat{E})\frac{1}{\mu_d}e^{(E-\hat{E})/\mu_d}d\hat{E} \tag{6}$$

The probability distribution for E after the subsequent upwards transition (step $2n + 2$) can be expressed as:

$$\hat{D}_{2n+2}(E) = \begin{cases} \int_{-\infty}^{E} D_{2n+1}(\hat{E})\frac{1}{\mu_c}e^{-(E-\hat{E})/\mu_c}d\hat{E} & E < 0 \\ \int_{-\infty}^{0} D_{2n+1}(\hat{E})\frac{1}{\mu_c}e^{-(E-\hat{E})/\mu_c}d\hat{E} & E \geq 0. \end{cases} \tag{7}$$

The corresponding probability that the subsequent charge will **not** replenish the battery is:

$$P_{2n+2} = \int_{-\infty}^{0} \hat{D}_{2n+2}(\hat{E})d\hat{E}. \tag{8}$$

Normalizing for $E < 0$ the distribution of energy levels of the subsequent charge is:

$$D_{2n+2}(E) = \frac{\hat{D}_{2n+2}(E)}{P_{2n+2}}. \tag{9}$$

Starting from ($n = 0$):

$$P_0 \stackrel{\triangle}{=} 1$$
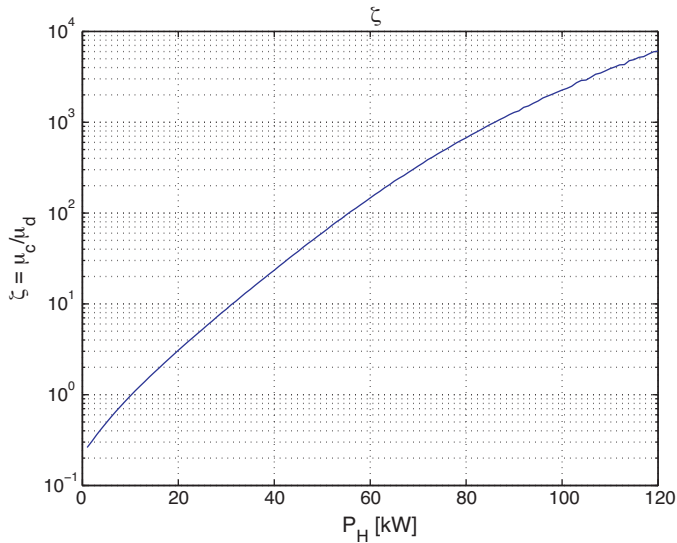
and

$$D_1(E) = \frac{1}{\mu_d}e^{E/\mu_d}$$

Fig. 8. $\zeta = \mu_c/\mu_d$ as a function of P_H.

we can calculate D_2 as:

$$\hat{D}_2(E) = \int_{-\infty}^{E} D_1(\hat{E}) \frac{1}{\mu_c} e^{(E-\hat{E})/\mu_c} d\hat{E} = \frac{1}{\mu_c + \mu_d} e^{E/\mu_d} \tag{10}$$

and

$$P_2 = \int_{-\infty}^{0} \hat{D}_2(\hat{E}) d\hat{E} = \frac{\mu_d}{\mu_c + \mu_d}$$

yielding:

$$D_2(E) = \frac{1}{\mu_d} e^{E/\mu_d}.$$

Calculating further D_3, D_4 and P_4 we get:

$$D_3(E) = \int_{E}^{0} D_2(\hat{E}) \frac{1}{\mu_d} e^{(E-\hat{E})/\mu_d} d\hat{E} = \int_{E}^{0} \frac{1}{\mu_d} e^{\hat{E}/\mu_d} \frac{1}{\mu_d} e^{(E-\hat{E})/\mu_d} d\hat{E} = \frac{E}{\mu_d^2} e^{E/\mu_d}$$

$$\hat{D}_4(E) = \int_{-\infty}^{E} \frac{\hat{E}}{\mu_d^2} e^{\hat{E}/\mu_d} \frac{1}{\mu_c} e^{-(E-\hat{E})/\mu_c} d\hat{E} = \frac{\mu_c}{(\mu_c + \mu_d)^2} e^{E/\mu_d} \left[1 - \left(\frac{1}{\mu_c} + \frac{1}{\mu_d}\right) E\right]$$

$$P_4 = \int_{-\infty}^{0} \hat{D}_4(\hat{E}) d\hat{E} = \int_{-\infty}^{0} \frac{\mu_c}{(\mu_c + \mu_d)^2} e^{\hat{E}/\mu_d} \left[1 - \left(\frac{1}{\mu_c} + \frac{1}{\mu_d}\right) \hat{E}\right] d\hat{E}$$

$$= \frac{\mu_c}{(\mu_c + \mu_d)^2} \int_{-\infty}^{0} e^{\hat{E}/\mu_d} d\hat{E} - \frac{\mu_c}{(\mu_c + \mu_d)^2} \left(\frac{1}{\mu_c} + \frac{1}{\mu_d}\right) \int_{-\infty}^{0} e^{\hat{E}/\mu_d} \hat{E} d\hat{E}$$

$$= \frac{\mu_d(2\mu_c + \mu_d)}{(\mu_c + \mu_d)^2}$$

Introducing the parameter $\zeta = \mu_c/\mu_d$, shown in Fig. 8, the lowest order P's are:

$$P_2 = \frac{1}{\zeta + 1}$$

$$P_4 = \frac{2\zeta + 1}{(\zeta + 1)^2}$$

$$P_6 = \frac{5\zeta^2 + 4\zeta + 1}{(2\zeta + 1)(\zeta + 1)^2}$$

$$P_8 = \frac{14\zeta^3 + 14\zeta^2 + 6\zeta + 1}{(\zeta + 1)^2 (5\zeta^2 + 4\zeta + 1)}$$

$$P_{10} = \frac{42\zeta^4 + 48\zeta^3 + 27\zeta^2 + 8\zeta + 1}{(\zeta + 1)^2 (14\zeta^3 + 14\zeta^2 + 6\zeta + 1)}$$

$$P_{12} = \frac{132\zeta^5 + 165\zeta^4 + 110\zeta^3 + 44\zeta^2 + 10\zeta + 1}{(\zeta + 1)^2 (42\zeta^4 + 48\zeta^3 + 27\zeta^2 + 8\zeta + 1)}$$

In general, the probability P_{2n} can be expressed as the ratio of two polynomials of ζ:

$$P_{2n} = \frac{\mathcal{N}_{2n}(\zeta)}{\mathcal{D}_{2n}(\zeta)}. \tag{11}$$

For a specific hybrid vehicle configuration, the parameter ζ is a function of P_H, as shown in Fig. 8 for our example vehicle. This parameter provides insight into the energy balance between discharge and charge events; higher values of ζ means that the energy used during discharge is more likely to be replenished in subsequent charge event. In contrast, smaller values of ζ (such as $\zeta < 1$) means that energy discharged is less likely be replenished. If ζ is too small, the charging events will not be able to keep up with the discharging events and the battery will eventually become totally discharged. This will occur if the primary source power (low P_H) rating is too low for the drive traces of interest.

If parameter α_{2n} is used to represent the coefficient of ζ^{n-1} in the polynomial $\mathcal{N}_{2n}$, then the inductive formula for P_{2n} that is true for all values of $n > 1$ can be written as:

$$P_{2n+2} = 1 - \frac{\alpha_{2n} \zeta^{n+1}}{(\zeta + 1)^2 \mathcal{N}_{2n}(\zeta)}. \tag{12}$$

The parameter α_{2n} is discussed further in Section 4.

The first several orders of D_{2n+1} are:

$$D_1 = \frac{e^{E/\mu_d}}{\mu_d}$$

$$D_3 = -\frac{Ee^{E/\mu_d}}{\mu_d^2}$$

$$D_5 = \frac{Ee^{E/\mu_d}(E + E\zeta - 2\mu_d\zeta)}{2\mu_d^3 (2\zeta + 1)}$$

$$D_7 = -\frac{Ee^{E/\mu_d}(E^2\zeta^2 + 2E^2\zeta + E^2 - 6E\mu_d\zeta^2 - 6E\mu_d\zeta + 12\mu_d^2\zeta^2)}{6\mu_d^4 (5\zeta^2 + 4\zeta + 1)}$$

$$D_9 = \frac{Ee^{E/\mu_d}}{24\mu_d^5 (14\zeta^3 + 14\zeta^2 + 6\zeta + 1)}(E^3\zeta^3 + 3E^3\zeta^2 + 3E^3\zeta + E^3$$
$$- 12E^2\mu_d\zeta^3 - 24E^2\mu_d\zeta^2 - 12E^2\mu_d\zeta + 60E\mu_d^2\zeta^3 + 60E\mu_d^2\zeta^2$$
$$- 120\mu_d^3\zeta^3)$$

$$D_{11} = -\frac{Ee^{E/\mu_d}}{720\mu_d^7 (132\zeta^5 + 165\zeta^4 + 110\zeta^3 + 44\zeta^2 + 10\zeta + 1)}(E^5\zeta^5$$
$$+ 5E^5\zeta^4 + 10E^5\zeta^3 + 10E^5\zeta^2 + 5E^5\zeta + E^5 - 30E^4\mu_d\zeta^5$$
$$- 120E^4\mu_d\zeta^4 - 180E^4\mu_d\zeta^3 - 120E^4\mu_d\zeta^2 - 30E^4\mu_d\zeta$$
$$+ 420E^3\mu_d^2\zeta^5 + 1260E^3\mu_d^2\zeta^4 + 1260E^3\mu_d^2\zeta^3 + 420E^3\mu_d^2\zeta^2$$
$$- 3360E^2\mu_d^3\zeta^5 - 6720E^2\mu_d^3\zeta^4 - 3360E^2\mu_d^3\zeta^3$$
$$+ 15,120E\mu_d^4\zeta^5 + 15,120E\mu_d^4\zeta^4 - 30,240\mu_d^5\zeta^5)$$

The distributions D_{2n+1} can be calculated ($n \geq 1$) using:

$$D_{2n+1}(E) = \frac{(-1)^n Ee^{E/\mu_d}}{n!\mu_d^{n+1} \mathcal{N}_{2n}(\zeta)} \sum_{k=0}^{n-1} \left[(-1)^k \frac{(n+k-1)!}{k!(n-k-1)!} (E(\zeta+1))^{n-k-1} \mu_d^k \zeta^k\right] \tag{13}$$

The first few P parameters as a function of P_H calculated based on drive profile for our example vehicle are shown in Fig. 9.

Going back to Eqs. (3) and (12), and realizing that after canceling terms from the multiplication of the P terms

$$\prod_{j=1}^{n} P_{2j}(\zeta) = \frac{\mathcal{N}_{2n}(\zeta)}{(\zeta + 1)^{2n-1}} \sim \frac{1}{(\zeta + 1)^n}. \tag{14}$$

where $\mathcal{N}_{2n}(\zeta)$ is defined in Eq. (11). We note that $\hat{D}(E)$ can be written as:

$$\hat{D}(E) = D_1(E) + \sum_{n=1}^{\infty} \left(D_{2n+1}(E) \frac{\mathcal{N}_{2n}(\zeta)}{(\zeta + 1)^{2n-1}}\right). \tag{15}$$

Fig. 9. P_{2n} as a function of P_H.

Using Eq. (13) and rearranging the terms it becomes:

$$\hat{D}(E) = \frac{e^{E/\mu_d}}{\mu_d} \left\{ 1 + \sum_{n=1}^{\infty} \left[(-1)^n \sum_{k=0}^{n-1} \left[\frac{(n+k-1)!}{k!n!(n-k-1)!} \frac{(-\zeta)^k}{(\zeta+1)^{n+k}} \left(\frac{E}{\mu_d} \right)^{n-k} \right] \right] \right\}$$

After normalization, the normalized distribution $D(E)$ can be written as:

$$D(E) = \frac{e^{E/\mu_d}}{\mu_d} \frac{\left\{ 1 + \sum_{n=1}^{\infty} \left[(-1)^n \sum_{k=0}^{n-1} \left[\frac{(n+k-1)!}{k!n!(n-k-1)!} \left(\frac{E}{\mu_d} \right)^{n-k} \frac{(-\zeta)^k}{(\zeta+1)^{n+k}} \right] \right] \right\}}{\sum_{n=1}^{\infty} \left[\frac{\mathcal{N}_{2n}(\zeta)}{(\zeta+1)^{2n-1}} \right]}$$

The cumulative distributions of $D(E)$ as function of P_H for our demonstration vehicle are shown in Fig. 10. Each contour on this graph represents a specific probability that the battery will reach a certain energy level after a discharge event. For example the energy level in the battery will be below or to the right of the line marked

Fig. 10. $D(E)$ for various P_H.

0.68269 after 68.269% of discharge events. We can see that in this case, when the primary power supply is larger than 75 kW the contours are nearly vertical. This means that the size of the primary power supply has almost no impact on the distribution of energy in the battery.

It can also be seen that for $P_H \approx 10$ kW ($\zeta = 1$ point) the contour lines become horizontal meaning that the energy capacity requirement increases (almost) indefinitely. As mentioned before, $\zeta = 1$ is limiting case below which the primary power source is not capable of replenishing the energy used.

4. Parameter α

Introduced in Eq. (12) as the coefficient associated with $n-1$ power of ζ in the polynomial $\mathcal{N}_{2n}$, the parameter α_{2n} deserves a closer look, especially since it is not dependent on ζ. From Eq. (12) for $n \geq 1$:

$$\mathcal{D}_{2n+2}(\zeta) = (\zeta + 1)^2 \mathcal{N}_{2n}(\zeta)$$

and

$$\mathcal{N}_{2n+2}(\zeta) = \mathcal{D}_{2n+2}(\zeta) - \alpha_{2n}\zeta^{n+1}.$$

Therefore, a recursive calculation for $\mathcal{N}_{2n}(\zeta)$, with initial values for $n = 0$, $\mathcal{N}_2(\zeta) = 1$, and $\alpha_0 = 1$, can be expressed as:

$$\mathcal{N}_{2n+2}(\zeta) = (\zeta + 1)^2 \mathcal{N}_{2n}(\zeta) - \alpha_{2n}\zeta^{n+1}. \tag{16}$$

Now, denoting the coefficients of the polynomial $\mathcal{N}_{2n}(\zeta)$ as $a_{n,i}$ with $i = 0 \ldots n-1$,

$$\mathcal{N}_{2n}(\zeta) = \sum_{k=0}^{n-1} a_{n,n-k-1}\zeta^k.$$

Noting that $\alpha_{2n} = a_{n,0}$, the dependency of the coefficients of the $\mathcal{N}_{2n+2}(\zeta)$ can be written as:

$$a_{n+1,j} = a_{n+1,j-1} + 2a_{n,j} + a_{n,j+1}$$

with the exception of (after term $\alpha_{2n}\zeta^{n+1}$ is canceled):

$$a_{n+1,0} = \alpha_{2n+2} = 2a_{n,0} + a_{n,1} = 2\alpha_{2n} + a_{n,1}. \tag{17}$$

Defining the tridiagonal $n \times n$ matrix $\mathfrak{G}$ ($\mathfrak{G} = \text{tridiag}(1, 2, 1)$) as:

$$\mathfrak{G} = \begin{bmatrix} 2 & 1 & 0 & 0 & \cdots & 0 & 0 & 0 & 0 \\ 1 & 2 & 1 & 0 & \cdots & 0 & 0 & 0 & 0 \\ \vdots & \vdots & \vdots & \vdots & \ddots & \vdots & \vdots & \vdots & \vdots \\ 0 & 0 & 0 & 0 & \cdots & 1 & 2 & 1 & 0 \\ 0 & 0 & 0 & 0 & \cdots & 0 & 1 & 2 & 1 \\ 0 & 0 & 0 & 0 & \cdots & 0 & 0 & 1 & 2 \end{bmatrix}$$

the coefficients of polynomial $\mathcal{N}_{2n}(\zeta)$ can be calculated as:

$$\begin{bmatrix} a_{n,0} \\ a_{n,1} \\ \vdots \\ a_{n,n-1} \end{bmatrix} = \mathfrak{G}^{n-1} \begin{bmatrix} 1 \\ 0 \\ \vdots \\ 0 \end{bmatrix}. \tag{18}$$

Calculating powers of $\mathfrak{G}$ using methods described in Refs. [19,20], is straight forward. Of particular interest is $\alpha_{2n} = a_{n,0}$ that can be expressed as:

$$\alpha_{2n} = \frac{4(2n-1)}{2n+2}\alpha_{2n-2} = \frac{4^{n+1}(2n-1)!!}{2(2n+2)!!} \tag{19}$$

Some coefficients that are easily calculated are $a_{n,n-1} = 1$ and $a_{n,n-2} = 2n$.

5. Special case $\zeta = 1$

This case is singled out because it is the limiting case between converging and diverging energy distributions. For this value of ζ the distributions for charge and discharge are the same. In this case the energy state may eventually return to its initial state, but the number of high order excursions becomes significant, and mathematically speaking convergence of $D(E)$ cannot be guaranteed. For that reason, it deserves closer look.

Using $\zeta = 1$, we can expand the transition probabilities P as:

$$P_2 = \frac{1}{2} \qquad P_4 = \frac{3}{4}$$
$$P_6 = \frac{10}{12} \qquad P_8 = \frac{35}{40}$$
$$P_{10} = \frac{126}{140} \qquad P_{12} = \frac{462}{504}$$

or after cancelation (in each case by the previous α_{2n} parameter, as described in Eq. (12)) the P's become:

$$P_2 = \frac{1}{2} \qquad P_4 = \frac{3}{4}$$
$$P_6 = \frac{5}{6} \qquad P_8 = \frac{7}{8}$$
$$P_{10} = \frac{9}{10} \qquad P_{12} = \frac{11}{12}$$

which can be written as:

$$P_{2n} = 1 - \frac{1}{2n} \tag{20}$$

An inductive proof is straight forward, using Eqs. (12) and (19). Using Eq. (12) we can write:

$$\alpha_{2n} = \frac{4 \mathcal{N}_{2n}(1)}{(2n+2)}. \tag{21}$$

and from Eqs. (19) and (21) we get:

$$\mathcal{N}_{2n+2}(1) = \left(\frac{1}{2}\right) 4^n \frac{(2n+1)!!}{(2n+2)!!} \tag{22}$$

6. Summary and conclusions

Based on Fig. 10, it is possible to approximate the minimum engine power (conventional internal combustion or any other alter-

native) and battery capacity based on an acceptable reliability limit. For example, the thick line in Fig. 10 represents a reliability level of only 3 instances out of one million discharge events would exceed the battery capacity. In an example of such a scenario, instead of providing 120 kW for 1 s the drivetrain would receive 80 kW for 1.5 s, which can be hardly noticeable by the driver.

Finally, it should be pointed out again that this proposed sizing method for hybrid powertrain is purely mathematical and does not take into consideration neither physical limitations (chemistry, capacitance, losses, degradation over time, etc.), nor vehicle requirements (acceleration, gradability, etc.).

References

[1] J.F. Donoghue, J.H. Bughart, Optimization Methods Applied to Hybrid Vehicle Design, Tech. rep., US Department of Energy, 1983.
[2] P. Atwood, S. Gurski, D.J. Nelson, K. Wipke, T. Markel, Future Car Congress, 2002.
[3] C. Schweinsberg, Hyundai Fuel-Cell Program Banks on Lithium-Based Batteries, WardsAuto.com, 2010.
[4] Toyota introducing $50k fuel cell car in 2015, Fuel Cell Dispatch, 2010.
[5] Fuel cells and diesel hybrids are future, says Zetche, SAE—Automotive Engineering International, 2008.
[6] Honda announces hybrids, but continues to eye fuel cell technology, http://www.fuelcelldispatch.com/AutomotivePower/, 2010.
[7] K. Osborne, M. Sulek, Convergence 2000 Society of Automotive Engineers, 2000.
[8] J. Adams, W. Yang, K. Oglesby, K. Osborne, SAE World Congress, 2000.
[9] T. Matsumoto, N. Watanabe, H. Siguira, T. Ishikawa, Electric Vehicle Symposium, vol. 18, 2001.
[10] M. Juraj, Fuel consumption optimization in parallel hybrid vehicle, http://www.posterus.sk, September 2009.
[11] A. Aneakawa, K. Yamamoto, SAE World Congress, 2009.
[12] N. Yamaguchi, A. Iwai, T. Fukushima, H. Shinoki, SAE World Congress, 2009.
[13] D. Friedman, SAE International Congress and Exposition, 2009.
[14] J.-Y. Park, Y.-K. Park, J.-H. Park, Proceedings of the Institution of Mechanical Engineers, Part D: Journal of Automobile Engineering (2008).
[15] D. Rizoulis, J. Burl, J. Beard, SAE World Congress, 2001.
[16] J. O'Rourke, M. Arcak, M. Ramani, Journal of Power Sources 187 (2009).
[17] H. Zhao, A. Burke, Journal of Power Sources 186 (2009).
[18] R. Smith, S. Shahidinejad, D. Blair, E. Bibeau, Transportation Research Part D (2011).
[19] L. Euler, Novi commenrarii academiae scientarium imperialis Petropolitanae, vol. XVIII, 1774, pp. 24–36.
[20] D. Salkuyeh, International Mathematical Forum, vol. 22, 2006, pp. 1061–1065.